

Application of bidirectional ellipsometry to the characterization of roughness and defects in dielectric layers

Thomas A. Germer

*Optical Technology Division
National Institute of Standards and Technology
Gaithersburg, Maryland 20899*

ABSTRACT

The polarization of light scattered into directions out of the plane of incidence is calculated for microroughness, defects, or particles in or near a dielectric film on a substrate. The theories for microroughness and Rayleigh scatter in the presence of dielectric films are reviewed, and a method for calculating the Mueller matrix for scatter from multiple sources is described. The situation of a 1 μm thick layer of SiO_2 on a silicon substrate illuminated by p -polarized 633 nm light at a 60° angle of incidence is used to demonstrate the model calculations. The polarization of scattered light is calculated for scatter from roughness at each of the interfaces separately and roughness of both interfaces when those roughnesses are correlated and uncorrelated. The scatter from a single Rayleigh defect is considered as a function of the position of that defect within the dielectric film, and the scatter from a random distribution of Rayleigh defects in the layer is calculated. The capability of distinguishing amongst different scattering sources is discussed.

Keywords: bidirectional ellipsometry, dielectric films, microroughness, polarimetry, scatter, defects, surfaces

1. INTRODUCTION

The polarization of light scattered by a number of materials has been demonstrated to enable the distinction amongst scattering resulting from microroughness, subsurface defects, and particulate contamination for the case of a single interface.¹ When light is directed onto a surface at an oblique angle with the electric field linearly polarized in the plane of incidence, light scattered into directions away from the specular direction has a polarization which is a signature of the scattering mechanism. For scatter into directions in the plane of incidence little information is gained, since isotropic scatterers will not rotate the polarization. However, out of the plane of incidence the polarization of the light reveals the location of the scattering source, be it above the surface, below the surface, or at the surface (in the case of microroughness). Experimental measurements have shown excellent agreement with the models.^{2,3}

Particle and defect detection on surfaces is often hampered by the presence of surface roughness.⁴ Since the polarization from microroughness is well defined, and the degree of polarization is high, a device can be built which collects light over most of the hemisphere, yet is blind to microroughness.⁵ Such a device can substantially improve the sensitivity for detecting particles and defects on rough surfaces. Diagnosing sources of scattered light is also possible by analyzing its polarization. In that manner, process conditions in a manufacturing environment can be readily monitored with a nondestructive tool at high speed.

The intensity of scattered light is a strong function of the size parameter of a defect. In the case of roughness, the amount of scattered light in a particular direction is proportional to the power spectral density function of the surface height modulations.^{4,6} For sufficiently small particles or defects, the scattered intensity varies as the sixth power of their diameter.⁷⁻⁹ The randomness associated with roughness also leads to spatial intensity variations,

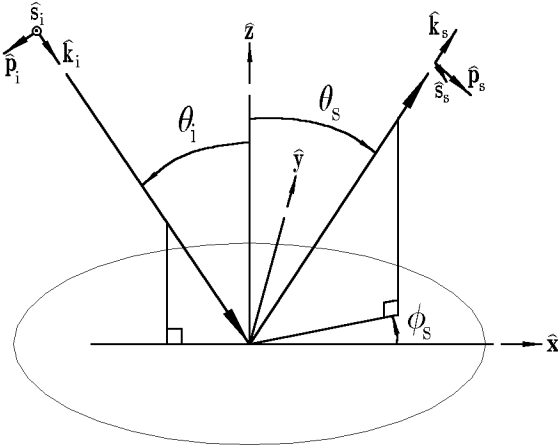


Figure 1 The sample coordinate system.

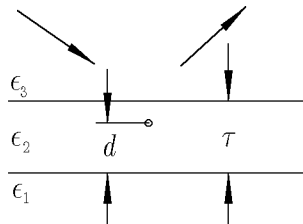


Figure 2 Diagram showing a layer of thickness τ and dielectric constant ϵ_2 surrounded by semi-infinite media of dielectric constants ϵ_1 and ϵ_3 . A small defect is located a distance d from the lower interface. Light is incident and collected from the top side.

usually referred to as speckle. Without undue disrespect to the information that is gained by the intensity, however, the polarization is a signature of the scattering source rather than its size. Furthermore, in the case of a single scattering source, the polarization is free of the rapid spatial variations characteristic of speckle. Therefore, in a process control or inspection application, where one wishes to identify the source of scatter, the polarization of scattered light can greatly aid the identification of defects.

We have chosen the term *bidirectional ellipsometry* to describe measurements whereby light is directed onto a surface with a fixed polarization state, and light scattered into directions away from the specular are analyzed by a rotating polarizing analyzer, yielding the angle η of the maximum signal (taken here to be with respect to *s*-polarized) and a degree of linear polarization P_L . Granted this technique is simply a restricted form of polarimetry, we prefer to use the term bidirectional ellipsometry, since the term eludes to its complementarity to bidirectional reflectance distribution function (BRDF) measurements and the similarities the technique has with specular ellipsometry. That is, bidirectional ellipsometry is to ellipsometry what bidirectional reflectance is to reflectance. This comparison begs a question: would bidirectional ellipsometry be as useful for characterizing defects in dielectric layers as specular ellipsometry is useful for characterizing the thicknesses of those layers?

In this paper, we extend previous work¹ to include scattering in systems with dielectric films in order to assess the application of bidirectional ellipsometry to the study of defects in those systems. In Sec. 2, we will describe the theoretical treatment for scattering from interfacial roughness and Rayleigh defects in a multilayer system. Included in Sec. 2 is a method for treating multiple sources, maintaining all of the polarimetric information. In Sec. 3, we will apply the theory to a 1 μm thick SiO_2 layer grown on silicon. In Sec. 4, we will summarize this work.

2. THEORY

Figure 1 shows the measuring geometry used for this discussion. Plane wave polarized light of wavelength λ irradiates the surface at an incident angle of θ_i in the plane defined by $\hat{\mathbf{x}}$ and $\hat{\mathbf{z}}$. We are interested in solving for the Jones or Mueller matrix for scattering into a direction defined by a polar angle θ_s and an out-of-plane angle ϕ_s . Unit vectors $\hat{\mathbf{k}}_i$ and $\hat{\mathbf{k}}_s$ describe the directions of propagation of the incident and scattered light, respectively. The polarization of the incident field is described by the components of the electric field along the $\hat{\mathbf{s}}_i$ and $\hat{\mathbf{p}}_i$ directions, where $\hat{\mathbf{s}}_i$ is a unit vector perpendicular to both $\hat{\mathbf{k}}_i$ and $\hat{\mathbf{z}}$, and $\hat{\mathbf{p}}_i = \hat{\mathbf{k}}_i \times \hat{\mathbf{s}}_i$. Likewise, the polarization of the scattered field in a particular direction is described by the components of the electric field along the $\hat{\mathbf{s}}_s$ and $\hat{\mathbf{p}}_s$ unit vectors, defined in an analogous manner as $\hat{\mathbf{s}}_i$, $\hat{\mathbf{p}}_i$, and $\hat{\mathbf{k}}_i$. We say that incident light is p -polarized (s -polarized) when it is linearly polarized with its electric field in the $\hat{\mathbf{p}}_i$ ($\hat{\mathbf{s}}_i$) direction.

The scattering (Jones) matrix J is defined as the relationship between the incident and scattered fields:

$$\begin{pmatrix} E_p^{\text{scat}} \\ E_s^{\text{scat}} \end{pmatrix} = \frac{\exp(ikR)}{R} \begin{pmatrix} J_{pp} & J_{sp} \\ J_{ps} & J_{ss} \end{pmatrix} \begin{pmatrix} E_p^{\text{inc}} \\ E_s^{\text{inc}} \end{pmatrix}, \quad (1)$$

where R is the distance from the scatterer to the detector, and $k = 2\pi/\lambda$. The matrix J can also be represented in its Mueller matrix form, $M = \mathcal{M}(J)$, where the operator \mathcal{M} is given by numerous texts.^{8,9} The Stokes vector associated with the scattered light, for p -polarized incident light, is then

$$S = \begin{pmatrix} S_1 \\ S_2 \\ S_3 \\ S_4 \end{pmatrix} = \begin{pmatrix} M_{11} - M_{12} \\ M_{21} - M_{22} \\ M_{31} - M_{32} \\ M_{41} - M_{42} \end{pmatrix}. \quad (2)$$

The angle η that the principle axis of the polarization ellipse makes with respect to the $\hat{\mathbf{s}}$ axis is related to the Stokes vector by

$$\eta = \arctan(S_2, S_3)/2. \quad (3)$$

The degree of polarization is

$$P = (S_2^2 + S_3^2 + S_4^2)^{1/2}/S_1, \quad (4)$$

while the degree of linear polarization is

$$P_L = (S_2^2 + S_3^2)^{1/2}/S_1. \quad (5)$$

In Sec. 2.A, we will consider scattering from interfacial microroughness, while we will devote Sec. 2.B to scattering that results from a very small sphere anywhere in a multilayer system. Lastly, in Sec. 2.C, we will present the formalism for including multiple scattering sources.

2.A. Interfacial microroughness

Elson described the solution to the first-order vector perturbation theory for scattering from interfacial microroughness in a dielectric stack.¹⁰⁻¹⁴ Since Ref. (10) is very explicit about how to carry out that calculation, we will not repeat its lengthy solution, but recognize that it can be readily programmed on a computer. However, we must make a few inferences to make it useful for this study.

The fractional power scattered per unit solid angle from the roughness of the n -th interface in a system with L layers, normalized to the incident power, while all the other interfaces are perfectly smooth, is found from Ref. (10) to be

$$\frac{1}{P_1} \frac{dP}{d\Omega} = \frac{\pi^2 \cos \theta_s}{\lambda^4 \cos \theta_i} \times \left[\left| \frac{A_p^{(n)}(\mathbf{k}_0 - \mathbf{k})}{P_{1,11}^{(1,L+1)}} \right|^2 + \left| \frac{A_s^{(n)}(\mathbf{k}_0 - \mathbf{k})}{S_{1,11}^{(1,L+1)}} \right|^2 \right], \quad (6)$$

where

$$A_p^{(n)}(\mathbf{k}_0 - \mathbf{k}) = \mu_p^{(n)} \Delta Z_n(\mathbf{k}_0 - \mathbf{k}), \quad (7)$$

and

$$A_s^{(n)}(\mathbf{k}_0 - \mathbf{k}) = \mu_s^{(n)} \Delta Z_n(\mathbf{k}_0 - \mathbf{k}). \quad (8)$$

The values of $P_{1,11}^{(1,L+1)}$, $S_{1,11}^{(1,L+1)}$, $\mu_p^{(n)}$, and $\mu_s^{(n)}$ are given in Ref. (10). The latter two values depend upon the angle ψ that the linearly polarized incident electric field makes with the plane of incidence. The Fourier transform of the roughness of the n -th interface is given by

$$\Delta Z_n(\mathbf{k}_0 - \mathbf{k}) = (1/A)^{1/2} \int_A d^2\mathbf{r} \Delta z_n(\mathbf{r}) \exp[i(\mathbf{k}_0 - \mathbf{k}) \cdot \mathbf{r}], \quad (9)$$

where $\Delta z_n(\mathbf{r})$ is the surface height function of the n -th layer about its mean value, and the integration is carried out over the irradiated area A . The vectors \mathbf{k}_0 and \mathbf{k} are the projections of $\hat{\mathbf{k}}_i$ and $\hat{\mathbf{k}}_s$ onto the xy plane, respectively, and are related to the scattering directions by

$$\begin{aligned} (\mathbf{k}_0 - \mathbf{k})_x &= k(\sin \theta_s \cos \phi_s - \sin \theta_i) \\ (\mathbf{k}_0 - \mathbf{k})_y &= k(\sin \theta_s \sin \phi_s). \end{aligned} \quad (10)$$

The two terms on the right hand side of Eq. (6) refer to the power scattered into p - and s -polarization, respectively. Since phases have otherwise been preserved in the paper, it is clear that the elements of the scattering matrix for interfacial microroughness are $S_{jk}^{\text{rough}} = [\pi^2 \cos \theta_s / (\lambda^4 \cos \theta_i)]^{1/2} q_{jk}^{\text{rough}} \Delta Z_n(\mathbf{k}_0 - \mathbf{k})$, where

$$\begin{aligned} q_{pp}^{\text{rough}} &= \mu_p^{(n)} \Big|_{\psi=0} / P_{1,11}^{(1,L+1)} \\ q_{sp}^{\text{rough}} &= -\mu_p^{(n)} \Big|_{\psi=\frac{\pi}{2}} / P_{1,11}^{(1,L+1)} \\ q_{ps}^{\text{rough}} &= \mu_s^{(n)} \Big|_{\psi=0} / S_{1,11}^{(1,L+1)} \\ q_{ss}^{\text{rough}} &= -\mu_s^{(n)} \Big|_{\psi=\frac{\pi}{2}} / S_{1,11}^{(1,L+1)}. \end{aligned} \quad (11)$$

The negative signs in Eq. (11) were chosen to guarantee that the results agreed with those of Rayleigh-Rice theory⁶ for a single interface.

2.B. Rayleigh defect in a multilayer system

In this section, we will present the results for a small spherical defect of radius a and dielectric constant ϵ_{sph} located between two interfaces. We assume that the defect is small enough that we can apply the Rayleigh approximation and that the scattered field from the defect does not interact with the defect a second time. Figure 2 illustrates the geometry used in this calculation. Using the approach outlined in Ref. (1), accounting for the existence of the two interfaces, we arrive at the scattering matrix elements $S_{ij}^{\text{def}} = q_{ij}^{\text{def}} S_0^{\text{def}}$, where

$$S_0^{\text{def}} = \epsilon_2^{5/4} \exp\{-i[q_2(\theta_s) + q_2(\theta_i)]d\} \left(\frac{\epsilon_{\text{sph}} - \epsilon_2}{\epsilon_{\text{sph}} + 2\epsilon_2} \right) a^3 k^2 \left[\frac{q_3(\theta_s)}{q_2(\theta_s)} \right]^{1/2} \quad (12)$$

and

$$\begin{aligned} q_{ss}^{\text{def}} &= t_s^{32}(\theta_i) t_s^{23}(\theta_s) \frac{B_s^{(+)}(\theta_s) B_s^{(+)}(\theta_i)}{C_s(\theta_s) C_s(\theta_i)} \cos \phi_s \\ q_{sp}^{\text{def}} &= -t_s^{32}(\theta_i) t_p^{23}(\theta_s) \frac{B_p^{(-)}(\theta_s) B_s^{(+)}(\theta_i)}{C_p(\theta_s) C_s(\theta_i)} \frac{q_2(\theta_s) \sin \phi_s}{k \epsilon_2^{1/2}} \\ q_{ps}^{\text{def}} &= -t_p^{32}(\theta_i) t_s^{23}(\theta_s) \frac{B_s^{(+)}(\theta_s) B_p^{(-)}(\theta_i)}{C_s(\theta_s) C_p(\theta_i)} \frac{q_2(\theta_i) \sin \phi_s}{k \epsilon_2^{1/2}} \\ q_{pp}^{\text{def}} &= t_p^{32}(\theta_i) t_p^{23}(\theta_s) \left[\frac{B_p^{(+)}(\theta_s) B_p^{(+)}(\theta_i)}{C_p(\theta_s) C_p(\theta_s)} \sin \theta_i \sin \theta_s - \frac{B_p^{(-)}(\theta_s) B_p^{(-)}(\theta_i)}{C_p(\theta_s) C_p(\theta_s)} \frac{q_2(\theta_s) q_2(\theta_i) \cos \phi_s}{k^2 \epsilon_2} \right]. \end{aligned} \quad (13)$$

The $B_j^{(\pm)}(\theta)$ and $C_j(\theta)$ factors are

$$\begin{aligned} B_j^{(\pm)}(\theta) &= 1 \pm r_j^{21}(\theta) \exp[2iq_2(\theta)d] \\ C_j(\theta) &= 1 - r_j^{23}(\theta)r_j^{21}(\theta) \exp[2iq_2(\theta)\tau], \end{aligned} \quad (14)$$

where $q_j(\theta) = k(\epsilon_j - \sin^2 \theta)^{1/2}$. The $r_\gamma^{\alpha\beta}(\theta)$ represent the reflection coefficients for γ -polarized light incident at an external angle θ traveling from region α to region β :

$$\begin{aligned} r_s^{\alpha\beta}(\theta) &= [q_\alpha(\theta) - q_\beta(\theta)]/[q_\alpha(\theta) + q_\beta(\theta)] \\ r_p^{\alpha\beta}(\theta) &= [\epsilon_\beta q_\alpha(\theta) - \epsilon_\alpha q_\beta(\theta)]/[\epsilon_\beta q_\alpha(\theta) + \epsilon_\alpha q_\beta(\theta)]. \end{aligned} \quad (15)$$

Likewise, the $t_\gamma^{\alpha\beta}(\theta)$ represent the transmission coefficients for γ -polarized light at an external angle θ traveling from region α to region β :

$$\begin{aligned} t_s^{\alpha\beta}(\theta) &= 2q_\alpha(\theta)/[q_\alpha(\theta) - q_\beta(\theta)] \\ t_p^{\alpha\beta}(\theta) &= 2(\epsilon_\alpha \epsilon_\beta)^{1/2} q_\alpha(\theta)/[\epsilon_\beta q_\alpha(\theta) + \epsilon_\alpha q_\beta(\theta)]. \end{aligned} \quad (16)$$

Although we derived Eqs. (12)–(14) for a defect in a single layer, the result is sufficiently general that we can calculate the scattering for a defect in a single layer within a multilayer stack straightforwardly, by recognizing that we can replace the reflection and transmission coefficients given in Eqs. (15) and (16) by the effective reflection coefficients of the layers above or below the layer of interest. Numerous texts on optics present transfer matrix methods which yield reflection and transmission coefficients for dielectric layers.⁷ Since a defect below all the layers is equivalent to letting $\epsilon_1 = \epsilon_2$, and a defect above all the layers is equivalent to letting $\epsilon_2 = \epsilon_3$, the Eqs. (12) and (13) are a more general form of Eqs. (15), (16), (23), and (24) of Ref. (1), which we derived for a particle above a single surface and a defect below a single surface.

2.C. Scattering from multiple sources

The field from different sources can add with some degree of coherence, depending upon the correlation between those scattering sources. For scalar quantities, it is well known that if several fields E_j are coherent, then they add as fields, that is, the intensity is

$$I_{\text{coh}} = \left| \sum_j E_j \right|^2.$$

If they are incoherent, the fields add as intensities, that is,

$$I_{\text{incoh}} = \sum_j |E_j|^2.$$

In general, each field has a random phase ϕ_j , so that the intensity I is given by

$$\begin{aligned} I &= \left| \sum_j E_j \exp(i\phi_j) \right|^2 \\ &= \sum_j \sum_k E_j^* E_k \exp[i(\phi_k - \phi_j)] \\ &= \sum_j |E_j|^2 + \sum_j \sum_{k < j} 2\text{Re}\{E_j^* E_k \exp[i(\phi_k - \phi_j)]\} \\ &= \sum_j |E_j|^2 + \sum_j \sum_{k < j} \left[2\text{Re}(E_j^* E_k) \text{Re}\{\exp[i(\phi_k - \phi_j)]\} - 2\text{Im}(E_j^* E_k) \text{Im}\{\exp[i(\phi_k - \phi_j)]\} \right] \\ &= \sum_j |E_j|^2 + \sum_j \sum_{k < j} \left[(|E_j + E_k|^2 - |E_j|^2 - |E_k|^2) \text{Re}\{\exp[i(\phi_k - \phi_j)]\} \right. \\ &\quad \left. + (|E_j + iE_k|^2 - |E_j|^2 - |E_k|^2) \text{Im}\{\exp[i(\phi_k - \phi_j)]\} \right]. \end{aligned} \quad (17)$$

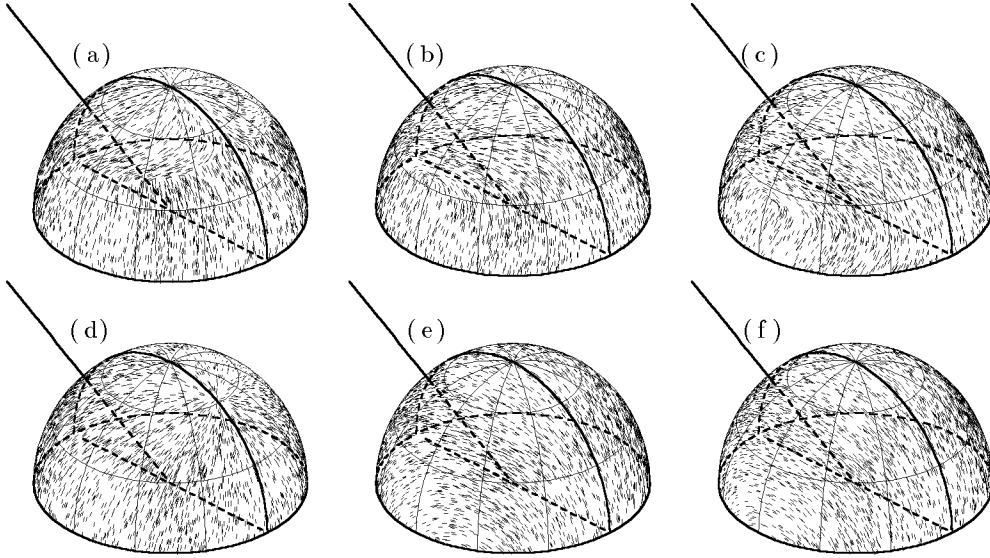


Figure 3 Polarization diagrams for scattering from different locations in a 1 μm thick SiO_2 layer grown on silicon for an incident angle of 60° and p -polarized incident light. The diagrams show the primary direction of the electric field, η , for a random distribution of directions on the scattering hemisphere. The defects are (a) a Rayleigh defect just above the SiO_2 layer, (b) roughness of the air/ SiO_2 interface, (c) a Rayleigh defect just below the air/ SiO_2 interface, (d) a Rayleigh defect just above the SiO_2 /silicon interface, (e) roughness of the SiO_2 /silicon interface, and (f) a Rayleigh defect in the silicon below all the interfaces.

By letting $I_j = |E_j|^2$, $I_{jk}^{(1)} = |E_j + E_k|^2$, $I_{jk}^{(2)} = |E_j + iE_k|^2$, and $c_{jk} = \langle \exp[i(\phi_j - \phi_k)] \rangle$, the average intensity for an arbitrary set of correlation parameters c_{jk} is

$$\langle I \rangle = \sum_j I_j + \sum_j \sum_{k < j} [(I_{jk}^{(1)} - I_j - I_k) \text{Re } c_{jk} + (I_{jk}^{(2)} - I_j - I_k) \text{Im } c_{jk}]. \quad (18)$$

We have assumed a scalar field in deriving Eq. (18). For scattering matrices, Eq. (18) still holds, provided we replace the intensities I_j , $I_{jk}^{(1)}$, and $I_{jk}^{(2)}$ by their Mueller matrix equivalents: $I_j \rightarrow \mathcal{M}(J_j)$, $I_{jk}^{(1)} \rightarrow \mathcal{M}(J_j + J_k)$, and $I_{jk}^{(2)} \rightarrow \mathcal{M}(J_j + iJ_k)$, where the Jones matrices for the j -th scattering source is J_j . Equation (18) is very practical for determining the Mueller matrix for a combination of scattering sources where the degree of coherence between the sources is known. For example, in Subsection 2.A, we described the scattering from a single rough interface in the presence of other smooth interfaces. We can readily calculate the Mueller matrices for scattering from multiple rough interfaces, be their roughnesses correlated, uncorrelated, partially correlated, or even anticorrelated, by applying Eq. (18).

3. RESULTS AND DISCUSSION

To demonstrate the results of the models presented in Section 2, we will consider a 1 μm thick SiO_2 layer grown on silicon. We will use a wavelength of 633 nm where the dielectric functions are assumed to be $\epsilon_{\text{oxide}}(633 \text{ nm}) = 2.25$ and $\epsilon_{\text{Si}}(633 \text{ nm}) = 15.07 + 0.015i$. Figure 3 shows the polarization pattern for scattering from six different sources, from each of the two interfaces and from each of four Rayleigh defects above and below each interface.

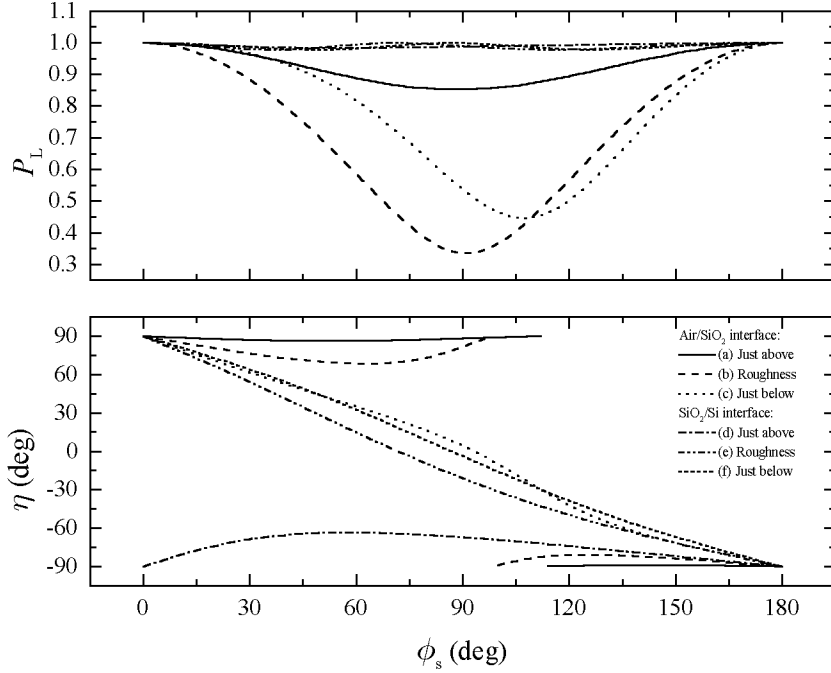


Figure 4 The parameters η and P_L for scattering from different locations in a $1 \mu\text{mSiO}_2$ layer grown on silicon. The incident and scattering angles are $\theta_i = \theta_s = 60^\circ$. The labeling and the conditions are similar to that for Fig. 3.

These diagrams show orthographic projections of the primary electric field vectors ($\hat{\mathbf{p}}_s \sin \eta + \hat{\mathbf{s}}_s \cos \eta$) over the unit hemisphere, in a manner similar to an iron filing diagram of a magnetic field. One can see from Fig. 3 that each scattering source yields a different pattern for the polarization. In the plane of incidence, the electric fields are always aligned in that plane, since by symmetry p -polarized light must scatter into p -polarized light in the plane of incidence. Therefore, the differences between the different source locations only yield differences in the polarization out of the plane of incidence.

Although the diagrams shown in Fig. 3 illustrate the differences between the different scattering mechanisms and can be a guide for choosing a specific geometry to study, they do not yield quantitative information. Figure 4 shows the model results for η and P_L for $\theta_i = \theta_s = 60^\circ$ for the same sample conditions as for Fig. 3. Since each of the curves in Fig. 4 represents a single mechanism, there are no sources of depolarization. Therefore, $P = 1$, and when $P_L < 1$, the scattered light has a degree of elliptical polarization. As seen in Fig. 3, each of the six situations leads to a different set of η and P_L curves. The differences between the curves for different sources are sufficiently great that a system with a 1° resolution should be able to distinguish between most of them. Two of the η curves, representing scattered light from cases (c) and (f) lie close to each other, yet their P_L are significantly different.

The large difference between cases (c) and (d) of Figs. 3 and 4 suggest that there is a strong dependence of the polarization of the scattered light on the position of the scatterer in the film. Figure 5 shows the dependence of η and P_L on the location of the scatterer for the geometry $\theta_i = \theta_s = 60^\circ$ and $\phi_s = 90^\circ$. Oscillations in η , P_L , and S_1 of period $l = \lambda q_2(\theta_i)/(2k)$ result from the interference between each interface. The strict periodicity of those oscillations is a result of $\theta_i = \theta_s$; for $\theta_i \neq \theta_s$, interference between two periods can be observed. The polarization properties of the scattered light are constant in the bulk material, since no interference exists.

If a large number of defects exist in the dielectric film, then only under unusual conditions would they all have a single value of d . Therefore, we must integrate the Mueller matrix over the entire layer to arrive at the

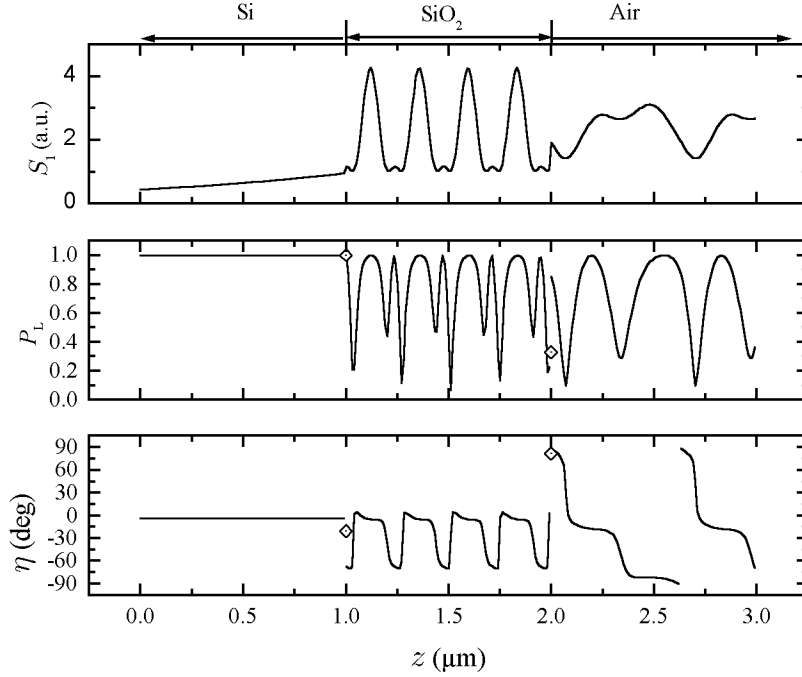


Figure 5 The parameters η , P_L , and S_1 for scattering from different locations near a $1 \mu\text{m}$ SiO_2 layer grown on silicon. The incident and scattering angles are $\theta_i = \theta_s = 60^\circ$ and the out-of-plane angle is 90° . The lines represent the positional dependence of a Rayleigh scatterer, while the symbols represent roughness at one of each of the two interfaces. The scales for S_1 are arbitrary between each layer.

incoherently-summed net Mueller matrix. When averaging through the thickness of the oxide layer, we achieve values of $\eta = -7.2^\circ$ and $P_L \approx P = 0.727$. This value of η is very similar to the value for scattering in the bulk, where the model predicts $\eta = -3.7^\circ$ and $P_L = P = 1$. That this average does not correspond to the direct averages of η (-51.2°) and P_L (0.765) is due to the fact that the intensity of the scattered light, S_1 , is not constant with position in the film (see Fig. 5). Figure 6 shows the dependence of the layer average on ϕ_s for defects in the bulk material and in the dielectric layer. The two η curves lie close to each other, suggesting that it may be difficult to distinguish between defects in the bulk material and defects randomly dispersed in the dielectric film, at least for the $1 \mu\text{m}$ film and optical geometry considered here. Although we can distinguish them by their degree of polarization, we must be cautious of this conclusion, since in a real film other sources of depolarization may exist.

The strong dependence of the polarization of the scattered light outside of the material (see Fig. 5) has a potentially powerful application. Generally, the amplitude of light scattered by a particle (when it is sufficiently small) provides insufficient information to determine both its size and its material. The interference behavior outside of the material suggests that a larger particle can be distinguished from a smaller one by the polarization of the scattered light, since the size of a particle determines its mean distance from the surface. Hence, by knowing the quantity of light scattered, the index of refraction of the material can be estimated. This result is not dependent upon the existence of the dielectric layer, but relies instead upon interference between the incident and reflected light.

Figure 7 outlines the ellipsometric parameters for scattering due to roughness of the interfaces, where the individual contributions from each of the two interfaces are shown with the correlated and uncorrelated sums of both together as a function of ϕ_s for $\theta_i = \theta_s = 60^\circ$. The amplitude of the roughness is assumed to be the same for

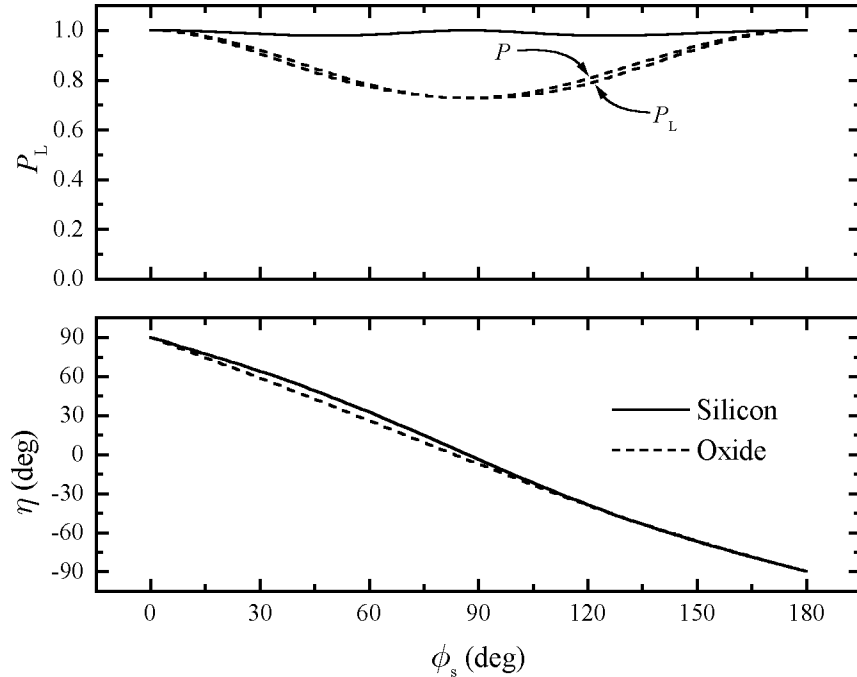


Figure 6 The parameters η and P_L for scattering from a random distribution of Rayleigh defects in the silicon and in the oxide. The incident and scattering angles are $\theta_i = \theta_s = 60^\circ$.

each interface. Since the change of the dielectric function is larger for the SiO_2/Si interface than for the air/SiO_2 interfaces, the intensity of scattered light from the air/SiO_2 interface is substantially smaller. For that reason, one observes that η for the uncorrelated sum is similar to that for the SiO_2/Si interface signal. When the fields add coherently, however, the presence of the second interface has a much stronger contribution, as is indicated by the substantial difference between the correlated sum and any of the other curves.

All of the cases shown in Fig. 7, except the uncorrelated one, yield $P = 1$, since they have no random variables and hence no depolarization mechanism. Therefore, each of these P_L curves indicates a degree of circular polarization. For the incoherent sum, we show both P_L and P , indicating the presence of depolarized scattered light.

If the roughness results from “feedthrough” of the roughness of the bottom layer onto the top layer during the growth process, we may suppose that for roughness wavelengths much larger than the layer thickness some degree of correlation would exist, and that for thicknesses much larger than the roughness wavelength that the opposite would hold true. Since the magnitude of the spatial frequency for $\theta = \theta_i = \theta_s$ is $f = 2 \sin \theta \sin(\phi_s/2)/\lambda$, we can make an estimate of the out-of-plane angles where correlation would be expected. Under the assumption of feedthrough roughness, and for a $1 \mu\text{m}$ film, incident and scattering angles $\theta_i = \theta_s = 60^\circ$, and wavelength $\lambda = 633 \text{ nm}$, one might expect that out-of-plane angles $\phi_s < 43^\circ$ should be correlated. Other roughness mechanisms will yield different results. For example, a nonuniform growth mechanism will generate a lack of correlation at low spatial frequencies. Bidirectional ellipsometry can potentially be used to measure the correlation function between two interfaces of a dielectric layer if other scattering mechanisms do not exist. In such a measurement, the roughness of at least one of the interfaces must be determined independently, such as with a scanning probe microscopy.

In order to keep this article to a reasonable length, we considered only a limited number of optical geometries and only one sample arrangement. It is worthwhile to make a few comments about other situations. For the

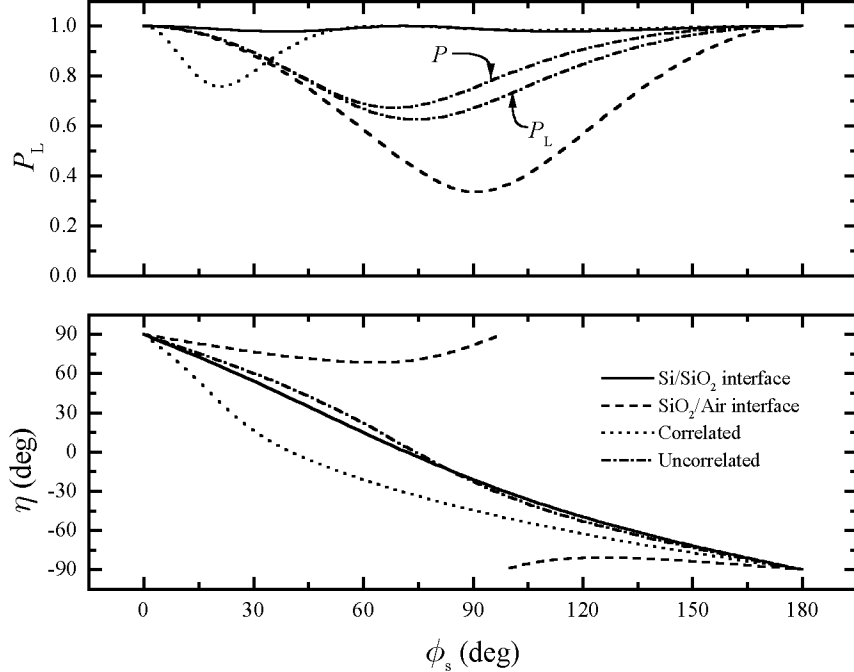


Figure 7 The parameters η and P_L for scattering from roughness of the 1 μm SiO₂ layer grown on silicon in the $\theta_i = \theta_s = 60^\circ$ geometry. Two curves are shown in the upper frame for the uncorrelated model, the upper one representing the parameter DOP.

measurement geometry, we chose to use p -polarized incident light since it tends to give the largest discrimination, especially for the case of a single interface. Other incident polarizations have their advantages as well. For example, 45° incident polarization allows measurements to be carried out in the plane of incidence. In this case, the contrast between one mechanism and another will result from differences in phase and amplitude between $s \rightarrow s$ and $p \rightarrow p$ scattering, in much the same way as traditional specular ellipsometry uses the phase and amplitude changes between s and p reflection to gain information about surfaces. Likewise, one can use p -polarized incident light and measure the degree and sign of circular polarization in out-of-plane directions. For those mechanisms which predict some degree of elliptically polarized light, these configurations may yield some useful discrimination; however, many mechanisms yield linearly polarized light, making this geometry incapable of discrimination.

We also chose to concentrate on measurement geometries for which θ_i and θ_s are held constant and equal to each other. This class of geometries has the advantage that roughness over a wide range of spatial frequencies can be measured, since the specular beam is included (at $\phi_s = 0$). Furthermore, by reducing the number of degrees of freedom in a single measurement, the amount of data is reduced to a manageable level.

Although we chose to study a particular sample, the models are applicable to a wide range of different materials, including different dielectrics and thicknesses on silicon, coatings on transparent or reflecting optics, and protective coatings on materials. For most of these systems, provided that the optical constants of the materials involved are known, a similar set of results will be obtained.

4. SUMMARY

In this paper, we have presented models for polarized light scattering from interfacial roughness and small spheres in one or more dielectric layers. Furthermore, we have derived an expression for determining the Mueller

matrix when a number of scattering sources exist and where the degree of correlation between those sources is known. To illustrate the application of these models, we considered a 1 μm thick SiO_2 layer grown on silicon. We evaluated these models for the parameters η , P , and P_L in the geometry $\theta_i = 60^\circ$ using 633 nm p -polarized incident light. We find that scattering from each of six sources, roughness at each of the two interfaces and Rayleigh scattering above and below each interface, gives rise to a unique pattern for the polarization of the light scattered. We showed how light scattering from defects depends upon the position of the defect in the layer, and evaluated the ellipsometric parameters for a random distribution of defects in the layer, comparing the result for defects in the bulk material. We considered the scattering from roughness at both interfaces and found that the results were strongly dependent upon the correlation of the roughness, suggesting that measurements of the polarization of scattered light could be used to estimate the correlation function for roughness between two interfaces.

The technique of bidirectional ellipsometry should prove useful for analyzing light scattered by systems with dielectric layers. In most situations, the location of a scattering source can be determined. This capability will be useful for rapid analysis of materials, such as is needed for on-line quality control inspection of computer disks, semiconductor wafers, and flat panel displays.

REFERENCES

- [1] T. A. Germer, "Angular dependence and polarization of out-of-plane optical scattering from particulate contamination, subsurface defects, and surface microroughness," *Appl. Opt.* **36**, 8798–805 (1997).
- [2] T. A. Germer, and C. C. Asmail, "Bidirectional ellipsometry and its application to the characterization of surfaces," in *Polarization: Measurement, Analysis, and Remote Sensing*, D. H. Goldstein, and R. A. Chipman, ed., Proc. SPIE **3121**, 173–82 (1997).
- [3] T. A. Germer, C. C. Asmail, and B. W. Scheer, "Polarization of out-of-plane scattering from microrough silicon," *Opt. Lett.* **22**, 1284–6 (1997).
- [4] J. C. Stover, *Optical Scattering: Measurement and Analysis*, (McGraw-Hill, New York, 1990).
- [5] T. A. Germer, and C. C. Asmail, "Microroughness-blind hemispherical optical scatter instrument," Provisional U.S. Patent Application filed (1997).
- [6] D. E. Barrick, *Radar Cross Section Handbook*, (Plenum, New York, 1970).
- [7] M. Born, and E. Wolf, *Principles of Optics*, (Pergamon, Oxford, 1980).
- [8] H. C. v. d. Hulst, *Light Scattering by Small Particles*, (Dover, New York, 1981).
- [9] C. F. Bohren, and D. R. Huffman, *Absorption and Scattering of Light by Small Particles*, (Wiley, New York, 1983).
- [10] J. M. Elson, "Multilayer-coated optics: guided-wave coupling and scattering by means of interface random roughness," *J. Opt. Soc. Am. A* **12**, 729–42 (1995).
- [11] J. M. Elson, J. P. Rahn, and J. M. Bennett, "Light scattering from multilayer optics: comparison of theory and experiment," *Appl. Opt.* **19**, 669–79 (1980).
- [12] J. M. Elson, "Diffraction and diffuse scattering from dielectric multilayers," *J. Opt. Soc. Am.* **69**, 48–54 (1979).
- [13] J. M. Elson, "Infrared light scattering from surfaces covered with multiple dielectric overlayers," *Appl. Opt.* **16**, 2873–81 (1977).
- [14] J. M. Elson, "Light scattering from surfaces with a single dielectric overlayer," *J. Opt. Soc. Am.* **66**, 682–94 (1976).